Infrared emission spectroscopy and ab initio calculations on VCl[☆]

R.S. Ram,[a] J. Liévin,[b] P.F. Bernath,[a,c,*] and S.P. Davis[d]

[a] *Department of Chemistry, University of Arizona, Tucson, AZ 85721, USA*
[b] *Laboratoire de Chimie Physique Moléculaire, Université Libre de Bruxelles, CP 160/09, Av. F.D. Roosevelt 50, Bruxelles, Belgium*
[c] *Department of Chemistry, University of Waterloo, Waterloo, Ont., Canada N2L 3G1*
[d] *Department of Physics, University of California, Berkeley, CA 94720, USA*

Abstract

The emission spectrum of VCl has been investigated at high resolution in the 3000–19 400 cm^{-1} region using a Fourier transform spectrometer. The bands were excited in a high temperature carbon tube furnace by the reaction of vanadium metal vapor and a trace of BCl_3 as well as in a microwave discharge lamp by the reaction of $VOCl_3$ vapor with active nitrogen. The spectra were recorded using the Fourier transform spectrometer associated with the McMath–Pierce telescope of the National Solar Observatory at Kitt Peak. The analysis of the $E^5\Delta–X^5\Delta$ system of VCl (previously labeled as $[7.0]^5\Delta–X^5\Delta$) has been extended by analyzing the rotational structure of some additional bands. A rotational analysis of the $^5\Delta_1–^5\Delta_1$, $^5\Delta_3–^5\Delta_3$, and $^5\Delta_4–^5\Delta_4$ subbands of the 0–2, 0–1, 0–0, and 1–0 bands, and the $^5\Delta_2 - {}^5\Delta_2$ subband of the 0–1 and 0–0 bands has been obtained and molecular constants have been extracted. The $^5\Delta_{0\pm} - {}^5\Delta_{0\pm}$ subband was not identified in any of the assigned bands. The spectroscopic properties of the low-lying electronic states of VCl have been predicted by CASSCF/CMRCI ab initio calculations and the experimental assignments are supported by the ab initio results.
© 2003 Elsevier Science (USA). All rights reserved.

1. Introduction

Transition metal-containing molecules are species of importance in organic and organometallic chemistry [1–3]. Diatomic molecules such as VCl provide ideal models for the understanding of bonding and reactivity in transition metal systems [4]. Spectroscopic studies of these simple molecules are also of astrophysical importance. Because of the high abundance of transition metal elements on the surfaces of cool stars, several transition metal-containing diatomic oxides and hydrides have been identified [5–7] and there is strong possibility that the transition metal halide molecules may also be found. Precise spectroscopic data are necessary for a search for these species in complex stellar spectra. We have, therefore, initiated a program to study transition metal monohalides by analyzing their high resolution spectra in the near infrared and visible regions.

The emission spectrum of VCl was previously observed by Iacocca et al. [8] in the visible region. This spectrum consisted of only $\Delta v = 0$ sequence bands and no vibrational or rotational constants were obtained, and no conclusive electronic assignment was possible due to the lack of a rotational analysis. In a recent study of VCl, we have observed a complex $^5\Delta–^5\Delta$ transition in the near infrared which we labeled as the $[7.0]^5\Delta–X^5\Delta$ transition [9]. We also determined the spectroscopic constants from a rotational analysis of the 0–1 and 0–0 vibrational bands of this transition.

A number of visible bands of VF were observed at low resolution by Jones and Krishnamurty [10] and the electronic assignments of $^5\Sigma–^5\Pi$ or $^5\Delta–^5\Pi$ were proposed, although no rotational analysis was obtained. Recently a $^5\Delta–^5\Delta$ transition of VF has also been observed in the near infrared near 10 481 cm^{-1} and it has been labeled as $[10.5]^5\Delta–X^5\Delta$ on the basis of the rotational analysis of a few bands [11]. This transition is analogous to the $[7.0]^5\Delta–X^5\Delta$ system of VCl near 7000 cm^{-1}.

There is an ab initio calculation for the spectroscopic properties of the low-lying quintet states of VF which proposes a $^5\Delta$ ground state [12]. Recently ab initio cal-

Table 1
Rotational constants (in cm^{-1}) for the $X^5\Delta$ and $E^5\Delta$ states of VCl

Constants	$X^5\Delta_1$			$X^5\Delta_2$		
	$v = 0$	$v = 1$	$v = 2$	$v = 0$	$v = 1$	$v = 2$
T_{vv}	0.0	415.9120(36)	828.3174(29)	0.0	409.8683(26)	–
B_v	0.1652346(72)	0.1645294(75)	0.1637370(77)	0.165157(16)	0.164492(17)	–
$10^7 \times D_v$	1.151(11)	1.207(11)	1.282(15)	1.454(67)	1.811(68)	–
$10^3 \times q_v$	1.309(14)	1.262(14)	1.293(15)	0.7830(37)	0.8343(78)	–
$10^7 \times q_{Dv}$	−0.906(21)	−0.879(21)	−1.024(29)	−0.807(27)	−1.55(13)	–
$10^{11} \times q_{Hv}$	–	–	–	–	3.11(49)	–
Constants	$X^5\Delta_3$			$X^5\Delta_4$		
	$v = 0$	$v = 1$	$v = 2$	$v = 0$	$v = 1$	$v = 2$
T_{vv}	0.0	416.2039(26)	828.6948(27)	0.0	413.6719(20)	824.0845(18)
B_v	0.1656279(57)	0.1651175(60)	0.1644731(67)	0.1659329(39)9	0. 1653903(40)	0.1647921(42)
$10^7 \times D_v$	0.9694(74)	1.0168(88)	1.110(21)	1.1659(28)	1.1704(31)	1.1701(48)
$10^{12} \times H_v$	−1.573(27)	−0.551(32)	−0.53(29)	–	–	–
$10^9 \times q_{Dv}$	−1.754(35)	–	–	–	–	–
$10^{14} \times qH_v$	–	–	–	−6.17(11)	–	–
Constants	$E^5\Delta_1$			$E^5\Delta_2$		
	$v = 0$	$v = 1$		$v = 0$	$v = 1$	
T_{vv}	7001.9281(26)	7356.3330(13)		6941.7717(18)	–	
B_v	0.1533811(72)	0.1525339(74)		0.150852(16)	–	
$10^7 \times D_v$	1.044(11)	0.837(13)		−0.178(65)	–	
$10^4 \times q_v$	1.96(14)	2.92(14)		–	–	
$10^8 \times q_{Dv}$	−1.78(21)	0.43(23)		–	–	
Constants	$E^5\Delta_3$			$E^5\Delta_4$		
	$v = 0$	$v = 1$		$v = 0$	$v = 1$	
T_{vv}	6985.9660(17)	7340.1025(10)		6951.4111(14)	7305.1401(28)	
B_v	0.1547412(54)	0.1538611(56)		0.1562173(39)	0.1553695(69)	
$10^7 \times D_v$	1.2437(65)	1.0749(71)		1.7296(32)	1.798(34)	
$10^{12} \times H_v$	–	–		1.4047(79)	3.03(58)	

Note. Numbers in parenthesis are one standard deviation in the last digits.

culations have also been performed for VH by Bruna [13] and for VF by Harrison [14], and the spectroscopic properties for the low-lying electronic states have been predicted. The ground state of VF was predicted to be either the $^5\Delta$ or $^5\Pi$ state but no definite conclusion was drawn about which one was the lowest in energy [12]. On the other hand a $^5\Delta$ ground state was predicted for VH [13] on the basis of a high quality ab initio calculation by Bruna [13]. In general, transition metal halides and hydrides have very similar electronic structure suggesting that VF and VCl also probably have $^5\Delta$ ground states like VH [13].

In the present work we have extended the analysis of the near infrared transition of VCl by analyzing some additional bands primarily from a relatively cool microwave discharge source. A rotational analysis of the 0–2, 0–1, 0–0, and 1–0 bands has been obtained in the present work. Lines belonging to the $^5\Delta_1$–$^5\Delta_1$, $^5\Delta_2$–$^5\Delta_2$, $^5\Delta_3$–$^5\Delta_3$, and $^5\Delta_4$–$^5\Delta_4$ subbands have been measured. The rotational lines belonging to the $^5\Delta_{0\pm}$–$^5\Delta_{0\pm}$ subband could not be identified because of strong overlapping. The spectroscopic properties of the low-lying electronic states of VCl have also been predicted using ab initio calculations and our experimental assignments

are consistent with our ab initio results. Guided by the ab initio results we have decided to label the low-lying quintet states of VCl using the customary letter notation and the near infrared transition will, therefore, be labeled as $E^5\Delta$–$X^5\Delta$ in this paper.

2. Ab initio calculations

The low-lying electronic states of VCl (4 triplets and 7 quintets) have been characterized by means of large scale configuration interaction ab initio calculations. Their potential curves and the corresponding spectroscopic properties have been determined. All possible spin and spatial symmetries were investigated in order to characterize all the states lying below about 12 000 cm^{-1} with respect to the ground electronic state. The energy positions of the electronic states lying just above this limit were also located. In particular, the lowest states in the singlet and septet manifolds were investigated.

We refer to our previous work on transition metal-containing diatomic molecules [15–20] for details about the computational procedure adopted here and for an estimation of the accuracy of the calculated properties.

In brief, the procedure consists of a preliminary optimization of the molecular orbitals by state-averaged full-valence CASSCF calculations [21] followed by an internally contracted multireference configuration interaction (CMRCI) calculation [22] correlating all valence electrons. Davidson's correction [23] for four-particle unlinked clusters is added to the CMRCI energies. Both atoms are described by 10-core electron relativistic pseudopotentials and by the corresponding valence basis sets from the work of the Stuttgart group [24,25]. The molecular orbital (MO) space contains six σ, three π, and one δ MOs correlating with the $3s$, $3p$, $3d$, and $4s$ orbitals of vanadium and the $3s$ and $3p$ orbitals of chlorine. Three of these inner shell MOs (two σ and one π) were kept doubly occupied in all configurations. The number of active electrons involved in the correlation energy treatment is thus 12. The sizes of the CASSCF (CMRCI) wavefunctions range from 2100 to 5200 (350 000–700 000) configuration state functions (C_{2v} symmetry) depending on the space and spin symmetries. All calculations were performed with the MOLPRO package [26] running on the Compaq alpha servers of the ULB/VUB computer center.

3. Experimental

The VCl molecules were produced in two experiments. In the first experiment the molecules were observed by the reaction of V atoms with BCl_3 in a high temperature carbon tube furnace operated at a temperature of about 2200 °C. The details of the experimental setup used was provided in our previous VCl paper [9].

In the second experiment the VCl molecules were excited in an electrodeless microwave discharge in a flowing mixture of $VOCl_3$ vapor and active nitrogen, the details of which are provided in our recent publications on VO [27] and VN [28]. The spectra were recorded with the 1-m Fourier transform spectrometer associated with the McMath–Pierce telescope of the National Solar Observatory at Kitt Peak. The spectra in the 3400–19 400 cm^{-1} interval were recorded in two parts. For the 3400–14 700 cm^{-1} region the spectrometer was equipped with a CaF_2 beamsplitter, RG715 red pass filters and liquid nitrogen-cooled InSb detectors. The spectra were recorded by coadding four scans in about 1 h of integration at a resolution of 0.0156 cm^{-1}. For the 8700–19 400 cm^{-1} region, the spectrometer was equipped with a CaF_2 beamsplitter, OG530 filters, and midrange silicon diode detectors. The spectra in this region were recorded by coadding four scans in about 45 min of integration at a resolution of 0.025 cm^{-1}.

The spectral line positions were determined using a data reduction program called PC-DECOMP developed by J. Brault. The peak positions were determined by fitting a Voigt line shape function to each line. The furnace spectrum contained the vibration–rotation bands of HCl and HF as impurities in addition to the VF bands and V atomic lines. We have used the HF [29] line positions to calibrate our furnace spectra. The microwave discharge spectrum also contained VO and VN bands as well as V and He atomic lines. The CO $\Delta v = 2$ overtone sequence was present as impurity. The near infrared VCl spectrum from the microwave discharge source was calibrated using the measurements of the 2–0 overtone lines of CO provided by Maki [30]. The measurements of bands common to the spectra from the furnace and the microwave source were consistent within experimental error. The VCl rotational lines in the microwave discharge experiment appeared with a typical signal-to-noise ratio of 6:1 and have an approximate line width of 0.047 cm^{-1}. The expected absolute accuracy is about ± 0.003 cm^{-1}. The corresponding accuracy of measurements of strong and unblended lines from the furnace spectrum is expected to be of the order of ± 0.007 cm^{-1}.

4. Experimental results

In a previous publication we have reported on the rotational analysis of three subbands of the 0–1 and 0–0 bands of a near infrared transition of VCl [9]. These subbands were labeled as $^5\Delta_1$–$^5\Delta_1$, $^5\Delta_2$–$^5\Delta_2$, and $^5\Delta_3$–$^5\Delta_3$ and the transition was labeled as $[7.0]^5\Delta$–$X^5\Delta$. This assignment was based on the available theoretical results on VH [13] and VF [12]. At that time the remaining two subbands could not be identified because of strong overlapping in the furnace spectrum. In an attempt to better understand the electronic structure of VCl, a spectrum with higher resolution and a lower molecular temperature was analyzed. The bands in the new spectrum are still very complex because of overlapping from different subbands, but our Loomis–Wood program was very helpful in identifying the lines in the weaker bands. Using the new spectrum we were able to identify the rotational lines of a new subband (fourth subband). The structure of this subband consists of two R and two P branches. The rotational analysis of this subband indicates that the upper and lower states have Ω-doubling parameters smaller than those in the $^5\Delta_1$–$^5\Delta_1$ suband but larger than the values determined from the previously assigned $^5\Delta_2$–$^5\Delta_2$ subband. This has led us to revise the Ω assignments in two of the subbands analyzed previously [9]. From the analysis of the new subband we conclude that it is in fact the $^5\Delta_2$–$^5\Delta_2$ subband and the previous $^5\Delta_2$–$^5\Delta_2$ and $^5\Delta_3$–$^5\Delta_3$ subbands are the $^5\Delta_3$–$^5\Delta_3$ and $^5\Delta_4$–$^5\Delta_4$ subbands, respectively, of a $^5\Delta$–$^5\Delta$ transition. This electronic assignment is consistent with the results of our ab initio calculations discussed in the following section.

We have measured the rotational lines of the $^5\Delta_1$–$^5\Delta_1$, $^5\Delta_2$–$^5\Delta_2$, $^5\Delta_3$–$^5\Delta_3$, and $^5\Delta_4$–$^5\Delta_4$ subbands in the 0–2, 0–1, 0–0, and 1–0 bands, although the $^5\Delta_2$–$^5\Delta_2$ subband was identified only for the 0–1 and 0–0 bands and the $^5\Delta_{0\pm}$–$^5\Delta_{0\pm}$ subband was not identified at all. A compressed portion of the 0–1 band near the heads is presented in Fig. 1, where the R heads of the assigned subbands have been marked with arrows. As shown in Fig. 1, the subband positions do not follow any pattern based on increasing or decreasing Ω values, suggesting that the VCl states probably have case (c) characteristics. An expanded portion of $^5\Delta_3$–$^5\Delta_3$ subband of the

0–1 band is presented in Fig. 2, and some low-J, R, and P lines have been marked.

The rotational structure of each subband consists of R and P branches appearing with similar intensity indicating a $\Delta\Omega = 0$ assignment. The rotational constants for the different Ω states have been obtained by fitting the observed lines to the following energy level expression:

$$F_v(J) = T_v + B_v J(J+1) - D_v[J(J+1)]^2$$
$$+ H_v[J(J+1)]^3 \pm 1/2\{q_v J(J+1)$$
$$+ q_{Dv}[J(J+1)]^2 + q_{Hv}[J(J+1)]^3\}. \tag{1}$$

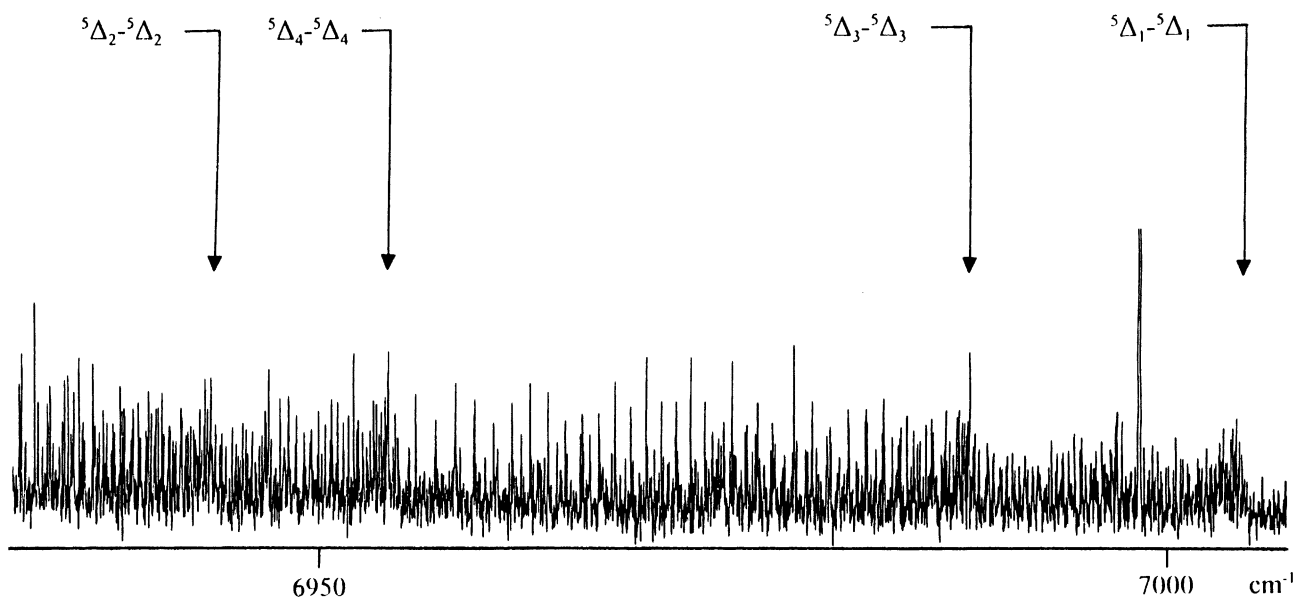

Fig. 1. A compressed portion of the 0–1 band of the $E^5\Delta$–$X^5\Delta$ transition of VCl with the assigned subband heads marked.
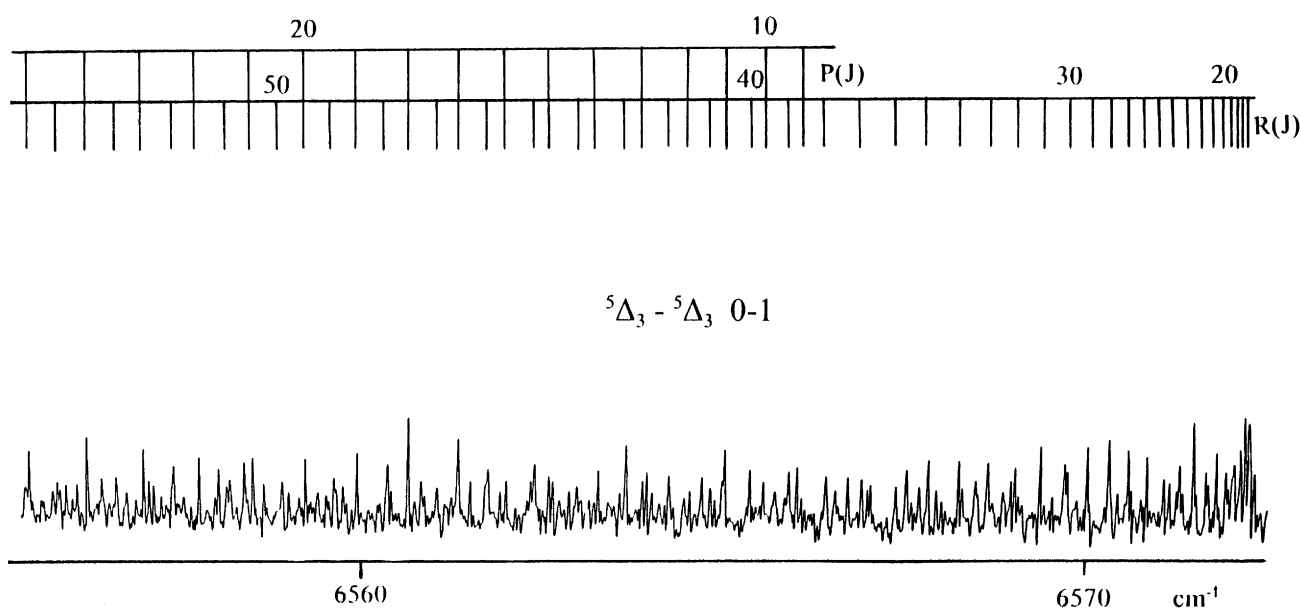

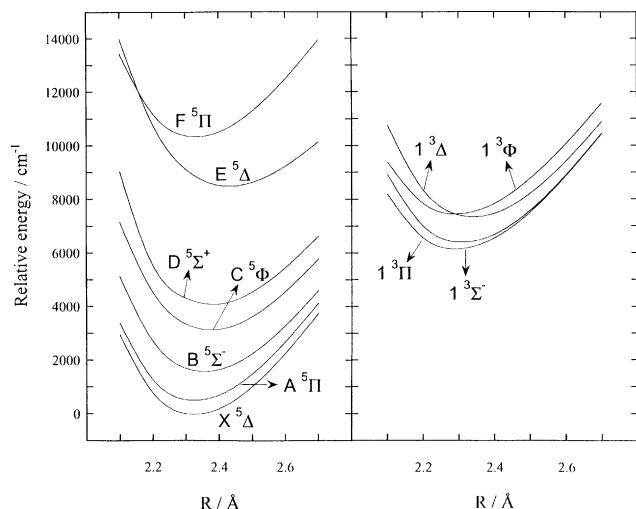Fig. 2. An expanded portion of the $^5\Delta_3$–$^5\Delta_3$ subband of the 0–1 band.

Fig. 3. The low-lying potential energy curves of VCl in the triplet and quintet spin systems from CMRCI calculations.

The rotational lines were weighted according to resolution and the extent of blending. The badly blended lines were heavily deweighted. The observed lines positions in the different bands can be obtained from the supplementary data available on-line [31] or from the authors upon request. The e/f parity assignment in the $^5\Delta_1$–$^5\Delta_1$ and $^5\Delta_2$–$^5\Delta_2$ subbands was made arbitrarily to provide a positive Ω-doubling constant q_v in the $X^5\Delta_1$ and $X^5\Delta_2$ spin components. The higher order Ω-doubling constants q_{Dv} and q_{Hv} were also determined for some vibrational levels of the ground state spin components and the $^5\Delta_1$ spin component of the $X^5\Delta$ state. The molecular constants for the different bands are provided in Table 5. Note that the Ω-doubling constants were not determined for the $^5\Delta_2$, $^5\Delta_3$, and $^5\Delta_4$ spin components of the excited state and were set to zero.

5. Electronic structure of VCl from ab initio calculations

The ab initio potential energy curves of the 11 low-lying electronic states of VCl are presented in Fig. 3, with the triplet and quintet states represented in two different panels. They have been obtained from CMRCI calculations performed at a set of internuclear distances ranging between 2.1 and 2.7 Å and separated by 0.1 Å. The energy scale is relative to the minimum energy of the ground electronic state. The spectroscopic properties calculated for all these states are given in Table 2. The following properties are reported: the equilibrium internuclear distances R_e, the harmonic frequencies at equilibrium ω_e and the term energies T_0, corrected for the zero point energy contribution calculated within the harmonic approximation.

The last column of Table 2 provides an analysis of the corresponding CMRCI wavefunctions in terms of a set of configurations, labeled from (A) to (J) and listed in Table 3. These configurations are those having a weight greater than or equal to 2% in the CMRCI wavefunctions, the weights being calculated as the sum of the squares of the CI coefficients of CSFs belonging to the corresponding electronic configurations. Configurations (A)–(F) can be considered as the leading configurations with weights greater than 70% in at least one of the calculated states, while configurations (G)–(J) are secondary configurations with weights below 20%. Also note that the numbering of the MOs in Table 3 refers to the valence orbitals only $\{1\sigma, 2\sigma, 1\pi, 3\sigma, 1\delta, 2\pi, 4\sigma\}$, occupied by the 12 so-called active electrons. The low energy structure of VCl thus arises, as shown in Table 3, from the distribution of the four "external" electrons in the MOs 3σ, 1δ, 2π, and 4σ. The total degeneracy of the resulting configurations is high, but the electrostatic splitting is large enough to limit the number of electronic

Table 2
Spectroscopic properties of the low-lying electronic states of VCl (from CMRCI calculations)

State	T_0 (cm^{-1})	R (Å)	ω_e (cm^{-1})	Configuration weights[a]
$X^5\Delta$	0	2.325	373	76% (A) + 17 % (F)
		(2.2145)	(417.4)	
$A^5\Pi$	517	2.326	366	62% (B) + 32% (D)
$B^5\Sigma^-$	1587	2.355	354	84% (C) + 10% (H)
$C^5\Phi$	3141	2.374	346	94% (D)
$D^5\Sigma^+$	4097	2.376	322	92% (E)
$1\,^3\Sigma^-$	6169	2.293	371	69% (C) + 14% (I) + 7 % (H)
$1\,^3\Pi$	6418	2.311	374	43% (B) + 20% (G) + 17% (D) + 5% (J)
$1\,^3\Delta$	7362	2.340	372	94% (A)
$1\,^3\Phi$	7470	2.293	362	48% (B) + 35% (D)
$E^5\Delta$	8494	2.430	321	17% (A) + 76 % (F)
	(7001.928)[b]	(2.2952)	(354.1)[c]	
$F^5\Pi$	10 356	2.332	369	29% (B) + 60% (D) + 4% (J)

Experimental values from this work are given in parentheses.
[a] Weights (in percentage) are obtained from the square of the corresponding configuration interaction coefficients; weights lower than 2% are not reported. See Table 3 for configuration labeling.
[b] T_{00} for the $E^5\Delta_1$–$X^5\Delta_1$ subband.
[c] $\Delta G_{1/2}$ value.

Table 3
Electronic configurations[a] describing the electronic states of VCl below 15 000 cm^{-1}

Labels	Configurations[a]
(A)	$3\sigma^1 1\delta^1 2\pi^2$
(B)	$3\sigma^1 1\delta^2 2\pi^1$
(C)	$3\sigma^1 1\delta^2 4\sigma^1$
(D)	$3\sigma^1 1\delta^1 2\pi^1\, 4\sigma^1$
(E)	$1\delta^2 2\pi^2$
(F)	$1\delta^1 2\pi^2 4\sigma^1$
(G)	$3\sigma^2 1\delta^1 2\pi^1$
(H)	$3\sigma^1 2\pi^2 4\sigma^1$
(I)	$3\sigma^2 1\delta^2$
(J)	$1\delta^2 2\pi^1 4\sigma^1$
(K)	$1\delta^2 4\sigma^2$
(L)	$3\sigma^1 2\pi^3$
(M)	$3\sigma^1 2\pi^1 4\sigma^2$
(N)	$3\sigma^2 1\pi^2$
(O)	$3\sigma^1 1\delta^3$
(P)	$3\sigma^1 1\delta^1 4\sigma^2$

[a] All configurations have the same closed shell structure $1\sigma^2 2\sigma^2 1\pi^4$. Configurations (K)–(P) contribute to states above 12 000 cm^{-1} only.

states to only 11 below 12 000 cm^{-1}. As expected, the highest spin states are more stable and the low-lying states of VCl belong to the quintet spin system, followed by the triplet system starting at about 6000 cm^{-1} (see Fig. 3). The singlet and septet systems were also investigated by CMRCI calculations, but are found to be out of the low-energy region. Both of these systems are located above 16 000 and 40 000 cm^{-1}, respectively. The vertical term energies of a few states in these systems were calculated at an internuclear distance of 2.3 Å, close to the equilibrium positions in VCl. The vertical energies of some quintet and triplet states above 12 000 cm^{-1} were also calculated. These results are reported in Table 4, together with the CMRCI configuration compositions. One sees that most of these states arise from the same set of leading configurations as

those occurring below 12 000 cm^{-1} (see Table 2), but with some additional secondary configurations, (K)–(L). The septet states require, however, the opening of the 2σ inner orbital, which explains the high values of the corresponding term energies.

The ground electronic state of VCl is thus predicted to be a $X^5\Delta$ state arising from configuration (A), $1\sigma^2 2\sigma^2 1\pi^4 3\sigma^1 1\delta^1 2\pi^2$, followed by a close-lying $A^5\Pi$ state from configuration (B), $1\sigma^2 2\sigma^2 1\pi^4 3\sigma^1 1\delta^2 2\pi^1$, and a $B^5\Sigma^-$ state from configuration (C), $1\sigma^2 2\sigma^2 1\pi^4 3\sigma^1 1\delta^2 4\sigma^1$. The next states in the quintet system ($C^5\Phi$ and $D^5\Sigma^+$) are not far away from the three low-lying ones. The two next states in this spin system are the second states of Δ and Π symmetry ($2^5\Delta$ and $2^5\Pi$). These two states which fall in the energy region of the observed spectrum are thus of particular interest. Referring to Table 4, one sees that no other quintet states have been characterized between 12 000 and 15 000 cm^{-1}, with the next quintet state being a $2^5\Sigma^-$ state at about 15 000 cm^{-1}.

The triplet manifold presents a set of four close-lying states ($1^3\Sigma^-$, $1^3\Pi$, $1^3\Phi$, and $1^3\Delta$) between 6000 and 7500 cm^{-1} and a second block ($1^3\Gamma$, $2^3\Pi$, $2^3\Sigma^-$, and $1^3\Sigma^+$) above 14 000 cm^{-1} (see Table 4). No other triplet state has been characterized within the gap separating the two triplet blocks.

It follows from the above ab initio survey of the low-lying electronic structure of VCl that the best candidates for the observed transition around 7000 cm^{-1} are from the pairs of close-lying states: $(E^5\Delta,\ F^5\Pi) \to (X^5\Delta,\ A^5\Pi)$. The transition dipole moments between these electronic states have been calculated at the CMRCI level of theory in order to assist in the assignment. We give in Table 5 the results obtained at an internuclear distance of 2.3 Å. Note that the signs of the transition moments are given as provided by MOLPRO. They are consistent with the phase choice of the CMRCI wavefunctions, which are build on a unique state-averaged orbital optimization. One finds that the $E^5\Delta \to X^5\Delta$ ($2^5\Delta \to 1^5\Delta$) transition is the most probable, with a

Table 4
Vertical term energies of some selected electronic states of VCl above 12 000 cm^{-1}, from CMRCI calculations ($R = 2.3$ Å)

2S+1	State	T_0 (cm^{-1})	Configuration weights [a]
1	$1^1\Sigma^+$	16 860	74% (I) + 15% (K)
	$1^1\Delta$	17 400	70% (I) + 13% (K) + 7% (N)
	$1^1\Pi$	18 270	75% (B) + 9% (D) + 4% (L) + 4% (M)
	$1^1\Phi$	18 135	51% (B) + 41% (D)
3	$1^3\Gamma$	14 090	71% (A) + 12% (O) + 9% (P)
	$2^3\Pi$	14 160	52% (B) + 39% (D)
	$2^3\Sigma^-$	14 780	66% (C) + 22%(A) + 4% (F)
	$1^3\Sigma^+$	14 960	85% (A) + 6% (C)
5	$2^5\Sigma^-$	15 300	83% (H) + 10% (C)
7	$1^7\Delta$	45 720	94% (Q)
	$1^7\Pi$	46 730	94 % (R)

[a] Weights (in percentage) are obtained from the square of the corresponding configuration interaction coefficients; weights lower than 2% are not reported.

Table 5
Matrix elements of the electric dipole moment operator (in debye) within the $1^5\Delta, 1^5\Pi, 2^5\Delta, 2^5\Pi$ set of states of VCl calculated from the CMRCI wavefunctions

States	$1^5\Delta$	$1^5\Pi$	$2^5\Delta$	$2^5\Pi$
$1^5\Delta$	5.78			
$1^5\Pi$	0.14	3.93		
$2^5\Delta$	2.01	0.38	5.24	
$2^5\Pi$	0.33	−0.84	0.64	4.10

large value of the transition dipole moment (2 D). The transition scheme is illustrated in Fig. 4, where the relative values of the square of the transition moments, with respect to the most intense transition, are indicated on the transition arrows. The final assignment of the observed transition can now be firmly made as the $E^5\Delta \rightarrow X^5\Delta$ transition.

The diagonal values of the electric dipole moment operator are also given in Table 5. The magnitude of these expectation values can be explained by the ionic character of VCl bond, which can be roughly depicted as $V^{\delta+}Cl^{\delta-}$, in which δ is the degree of molecular ionicity. One can evaluate the value of δ from a Mulliken atomic population analysis of the CASSCF wavefunctions. The values of δ obtained in this way are close to 0.65 for the $^5\Delta$ and $^5\Pi$ states, which is also close to the values calculated for the chlorides of the transition metals of the
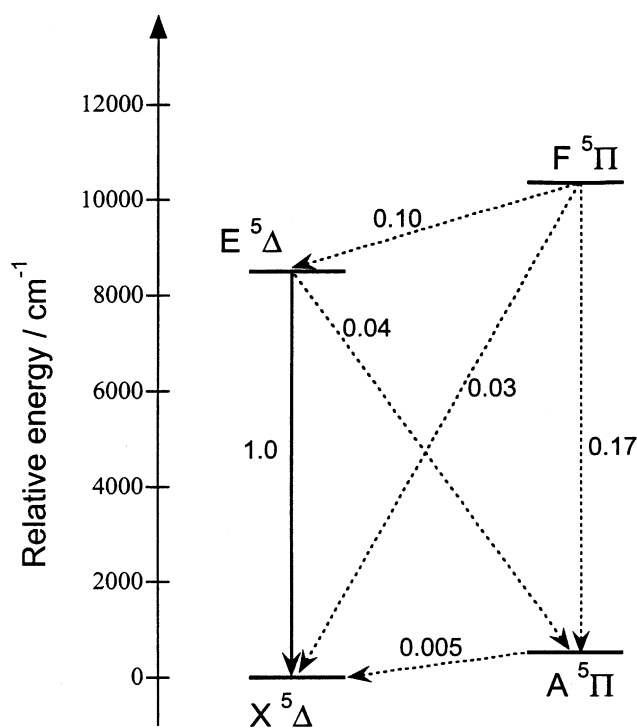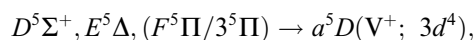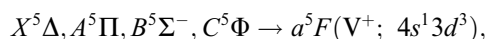
neighboring group IV B [19,20]. For instance the value of $\Delta = 0.68$ was obtained for the ground $X^4\Phi$ state of TiCl.

Electron populations on s, p, and d-type atomic orbitals centered on both atomic centers can also be derived from the Mulliken population analysis, making possible a correlation of the VCl states to those of the V^+ ion in the ligand field of Cl^-. Our ab initio results assign the X, A, B, and C states as arising from (V^+; $4s^1 3d^3$), but the D and E states come from (V^+; $3d^4$). As for the $F^5\Pi$ state, the predicted configuration on V^+ is close to $4s^{0.5}3d^{3.5}$, which indicates a strong configuration mixing. These results suggest the following correlation between the low-lying quintet states of VCl and those of isolated V^+ [32]:

$$X^5\Delta, A^5\Pi, B^5\Sigma^-, C^5\Phi \rightarrow a^5F(V^+;\ 4s^1 3d^3),$$

$$D^5\Sigma^+, E^5\Delta, (F^5\Pi/3^5\Pi) \rightarrow a^5D(V^+;\ 3d^4),$$

in which $(F^5\Pi/3^5\Pi)$ means that the $^5\Pi$ state involved in this correlation should mix with an upper $^5\Pi$ state bringing in some $4s^1 3d^3$ character. However, from an energetic point of view, the ground state of V^+ is the a^5D term, predicted [33] to be about 2800 cm^{-1} more stable than the a ^5F term. This inversion could mean that the effect of the ligand is to stabilize the $4s$ orbital, thus contributing more to the bonding than $3d$. Although there is some configuration mixing and shifting, the correspondence between the electronic states of VCl and those of V^+ is excellent.

One final comment on the electronic structure of VCl concerns the importance of electron correlation effects, and in particular the core-valence contributions. As pointed out above, three inner shell MOs (2σ and 1π) have been excluded from the CASSCF active space and were kept doubly occupied in all considered configurations. According to the CASSCF algorithm implemented in the MOLPRO package, there is no a priori constraint on the nature of the three molecular orbitals that will constitute this outer core (the only restriction being their symmetry). It is thus the variational procedure which will find the most stable solutions. In such transition metal-containing diatomic molecules, one would guess that these core MOs will directly correlate to the ns and np orbitals of the penultimate shell of the transition metal (i.e., the $3s$ and $3p$ orbitals on V in this case). This is indeed what we observed in our previous work on nitrides [15–17] and oxides [18]. The flexibility of the MCSCF procedure allows some degree of mixing between the orbitals of both atoms and in the case of VCl, there is a large contribution to these three orbitals from the chlorine atom. This means that the vanadium inner shells participate indirectly in the active space and introduce stabilizing correlation effects. Note that such core-valence correlation effects are well known in atomic calculations involving transition metals and their ions [32].

Fig. 4. Electronic transitions within the $X^5\Delta$, $A^5\Pi$, $E^5\Delta$, and $F^5\Pi$ states of VCl, from CMRCI calculations. The relative squares of the transition dipole moment with respect to the most intense transition are indicated on the arrows.

6. Discussion

The observation of several subbands in each band of the near infrared transition is consistent with the involvement of the high multiplicity states in the observed transition. The previously suggested $^5\Pi$ ground state assignment [12] for VF (or for VCl) is not consistent with the $^5\Delta$ ground state of VH [13] considering strong similarity between the transition metal halides and hydrides, although it may not be completely ruled out on this basis. Our $^5\Delta$ assignment for the ground state of VCl is on the other hand consistent with our own ab initio calculations and is also consistent with the high quality ab initio results for VH [13].

Although the rotational constants for the five spin components of the ground and excited states are not available because of severe overlapping, approximate Hund's case (a) equilibrium constants can be determined by simply averaging the rotational constants for the assigned spin components. These calculations provide $B_0 = 0.1655\,\text{cm}^{-1}$, $B_1 = 0.1649\,\text{cm}^{-1}$, and $B_2 = 0.1643\,\text{cm}^{-1}$ for the $X^5\Delta$ state. Using these values, the case (a) equilibrium constants of $B_e = 0.1658\,\text{cm}^{-1}$, $\alpha_e = 0.0006\,\text{cm}^{-1}$ have been determined for the $X^5\Delta$ state. Similarly the values of $B_0 = 0.1539\,\text{cm}^{-1}$ and $B_1 = 0.1530\,\text{cm}^{-1}$ have been obtained for the $E^5\Delta$ state, providing the equilibrium constants of $B_e = 0.1544\,\text{cm}^{-1}$ and $\alpha_e = 0.0009\,\text{cm}^{-1}$. These equilibrium rotational constants result in equilibrium bond lengths of $R''_e = 2.2145\,\text{Å}$ and $R'_e = 2.2952\,\text{Å}$ for the ground and excited states. These values can be compared with the ab initio bond lengths of $R''_e = 2.325\,\text{Å}$ and $R'_e = 2.430\,\text{Å}$. The constants of Table 5 have also been used to determine (by averaging) the approximate equilibrium vibrational constants of $\omega_e = 417.4\,\text{cm}^{-1}$, $\omega_e x_e = 3.5\,\text{cm}^{-1}$ for the ground state and $\Delta G'(1/2) = 354.1\,\text{cm}^{-1}$ for the excited state.

An inspection of the spectroscopic constants listed in Table 1 shows that the constants of the different spin components of the $X^5\Delta$ and $E^5\Delta$ states vary in an irregular manner. This is likely due to strong interaction with the close-lying $A^5\Pi$ and $D^5\Pi$ states. Although no local perturbations were observed over the range of observed J values, the highly unusual Ω-doubling seen in all four subbands indicates that the states are strongly mixed with the corresponding spin components of nearby $^5\Pi$ states. This argument is well supported by our ab initio calculations (Table 2). Our calculations show that the $A^5\Pi$ state lies at about $517\,\text{cm}^{-1}$ above the ground $X^5\Delta$ state. Similarly our ab initio calculations shows that the $F^5\Pi$ state lies about $1800\,\text{cm}^{-1}$ above the $E^5\Delta$ state. The microscopic form of the spin–orbit coupling operator has $\Delta\Omega = 0$ matrix elements between the two $(^5\Delta, {}^5\Pi)$ pairs of states so that all of the observed spin components (particularly for the lower state) have mixed Δ/Π character. Similar conclusions can be drawn

from the available theoretical studies on VF [12] and VH [13]. Averyanov and Khait [12] predict a $^5\Pi$ state at $1700\,\text{cm}^{-1}$ above the $X^5\Delta$ state for VF, while for VH [13] a $^5\Pi$ state is predicted at about $800\,\text{cm}^{-1}$ above the ground state. This is also consistent with the Harrison's theoretical predictions [14] for VF, which suggest very close-lying $^5\Delta$ and $^5\Pi$ lowest states.

7. Conclusions

The VCl molecules were excited in emission in a carbon tube furnace as well as in an electrodeless microwave discharge lamp, and the spectra have been recorded at high resolution using a Fourier transform spectrometer. Five groups of bands with R heads (for the highest wavenumber subband) near 6176, 6589, 7004, 7358, and $7710\,\text{cm}^{-1}$ have been assigned as the 0–2, 0–1, 0–0, 1–0, and 2–0 bands of the $E^5\Delta$–$X^5\Delta$ transition. A rotational analysis of the $^5\Delta_1$–$^5\Delta_1$, $^5\Delta_2$–$^5\Delta_2$, $^5\Delta_3$–$^5\Delta_3$, and $^5\Delta_4$–$^5\Delta_4$ subbands of various vibrational bands has been obtained and molecular constants have been extracted. The lower $X^5\Delta$ state of this transition has been assigned as the ground state of VCl. The experimental assignments of the observed states have been supported by our ab initio calculations of the spectroscopic properties of the low-lying electronic states of VCl.

Acknowledgments

References

[1] F.A. Cotton, G. Wilkinson, C.A. Murillo, M. Bochmann, Advanced Inorganic Chemistry, A Comprehensive Text, sixth ed., Wiley, New York, 1999.

[2] M. Grunze, in: D.A. King, D.P. Woodruff (Eds.), The Chemical Physics of Solid Surfaces and Heterogeneous Catalysis, vol. 4, Elsevier, New York, 1982, p. 143.

[3] F. Gassner, E. Dinjus, W. Leitner, Organometallics 15 (1996) 2078–2082.

[4] C.W. Bauschlicher Jr., S.P. Walch, S.R. Langhoff, Quantum Chemistry: The Challenge of Transition Metals and Coordination

Chemistry, in: A. Veillard (Ed.), NATO ASI Ser. C, Reidel, Dordrecht, 1986.

[5] O. Engvold, H. Wöhl, J.W. Brault, Astron. Astrophys. Suppl. Ser. 42 (1980) 209–213.

[6] B. Lindgren, G. Olofsson, Astron. Astrophys. 84 (1980) 300–303.

[7] R.S. Ram, P.F. Bernath, L. Wallace, Astrophys. J. Suppl. Ser. 107 (1996) 443–449.

[8] D. Iacocca, A. Chatalic, P. Deschamps, G. Pannetier, C.R. Acad. Sci., Paris C 271 (1970) 669–672.

[9] R.S. Ram, P.F. Bernath, S.P. Davis, J. Chem. Phys. 114 (2001) 4457–4460.

[10] W.E. Jones, G. Krishnamurty, J. Phys. B: Atom Mol. Phys. 13 (1980) 3375–3382.

[11] R.S. Ram, P.F. Bernath, S.P. Davis, J. Chem. Phys. 116 (2002) 7035–7039.

[12] A.S. Averyanov, Yu.G. Khait, Opt. Spectrosc. 67 (1990) 827–828.

[13] P.J. Bruna, private communication; J. Anglada, P.J. Bruna, S. Peyerimhoff, unpublished.

[14] J.F. Harrison, private communication.

[15] R.S. Ram, J. Liévin, P.F. Bernath, J. Chem. Phys. 109 (1998) 6329–6337.

[16] R.S. Ram, J. Liévin, P.F. Bernath, J. Mol. Spectrosc. 197 (1999) 133–146.

[17] R.S. Ram, J. Liévin, P.F. Bernath, J. Chem. Phys. 111 (1999) 3449–3456.

[18] R.S. Ram, J. Liévin, G. Li, T. Hirao, P.F. Bernath, Chem. Phys. Lett. 343 (2001) 437–445.

[19] R.S. Ram, A. Tsouli, J. Liévin, A. Adam, P. Bernath, J. Mol. Spectrosc. 202 (2000) 116–130.

[20] R.S. Ram, A.G. Adam, W. Sha, A. Tsouli, J. Liévin, P.F. Bernath, J. Chem. Phys. 114 (2001) 3977–3987.

[21] H.-J. Werner, P.J. Knowles, J. Chem. Phys. 82 (1985) 5053–5063; P.J. Knowles, H-J. Werner, Chem. Phys. Lett. 115 (1985) 259–267.

[22] H.-J. Werner, P.J. Knowles, J. Chem. Phys. 89 (1988) 5803–5814; P.J. Knowles, H.-J. Werner, Chem. Phys. Lett. 145 (1988) 514–522.

[23] S.R. Langhoff, E.R. Davidson, Int. J. Quantum Chem. 8 (1974) 61–74.

[24] M. Dolg, U. Wedig, H. Stoll, H. Preuss, J. Chem. Phys. 86 (1987) 866–872.

[25] A. Bergner, M. Dolg, W. Kuechle, H. Stoll, H. Preuss, Mol. Phys. 80 (1993) 1431–1441.

[26] MOLPRO (version 2000.1) is a package of ab initio programs written by H.-J. Werner, P.J. Knowles, with contributions from R.D. Amos, A. Bernhardsson, A. Berning, P. Celani, D.L. Cooper, M.J.O. Deegan, A.J. Dobbyn, F. Eckert, C. Hampel, G. Hetzer, T. Korona, R. Lindh, A.W. Lloyd, S.J. McNicholas, F.R. Manby, W. Meyer, M.E. Mura, A. Nicklass, P. Palmieri, R. Pitzer, G. Rauhut, M. Schütz, H. Stoll, A.J. Stone, R. Tarroni, T. Thorsteinsson.

[27] R.S. Ram, P.F. Bernath, S.P. Davis, A.J. Merer, J. Mol. Spectrosc. 211 (2002) 279–283.

[28] R.S. Ram, P.F. Bernath, S.P. Davis, J. Mol. Spectrosc. 210 (2001) 110–118.

[29] R.B. LeBlanc, J.B. White, P.F. Bernath, J. Mol. Spectrosc. 164 (1994) 574–579.

[30] A.G. Maki, J.S. Wells, Wavenumber Calibration Tables from Heterodyne Frequency Measurements, NIST Special Publication, vol. 821, US Government Printing Office, Washington, DC, 1999.

[31] Supplementary data can be found in the JMS electronic archive at http://www.apnet.com/www/journal/ms.htm or http://msa.lib.ohio-state.edu/jmsa_hp.htm.

[32] C.E. Moore, in: Atomic Energy Levels, vol. 1, National Bureau of Standards, Washington, DC, 1949.

[33] P. Quinet, J.E. Hansen, J. Phys. B: At. Mol. Opt. Phys. 28 (1995) L213–L220; J. Phys. B: At. Mol. Opt. Phys. 29 (1996) 1879.